Effect of Fluorinated Surface-Modifying Macromolecules on the Molecular Surface Structure of a Polyether Poly(urethane urea)

C. B. McCloskey,[†,‡] C. M. Yip,[†,‡] and J. P. Santerre*[,†,‡,§]

Department of Chemical Engineering and Applied Chemistry, University of Toronto, Toronto, Ontario, Canada M5G 1G6; Institute of Biomaterials and Biomedical Engineering, University of Toronto, Toronto, Ontario, Canada M5G 1G6; and Department of Biomaterials, Faculty of Dentistry, University of Toronto, Toronto, Ontario, Canada M5G 1G6

Received February 15, 2001; Revised Manuscript Received October 10, 2001

ABSTRACT: Fluorinated surface-modifying macromolecules (SMMs) have been developed to preferentially migrate to the surface of poly(urethane urea)s (PEUs), thereby modifying the surface features of the polymer. In the current study, four specific SMMs based on different chemistries were synthesized and incorporated at a 4 wt % concentration in the PEU. The domain structure at the surface was altered, and the nature of the interactions between the SMM and the base polymer was dependent on the defined SMM chemistry. The surface features were characterized by several microscopy techniques. Attenuated total reflectance infrared spectroscopy showed that, in blending with the PEU, some SMMs disrupted the existing hydrogen-bonded hard segment domain structure at the surface. However, this was not a necessity for good dispersion into the base polymer, as one SMM demonstrated good mixing within the PEU, forming SMM−PEU interactions while simultaneously maintaining the hydrogen bonding within the PEU hard segment domains. These studies demonstrate the importance of understanding both the physical and chemical aspects of the defined fluorinated SMM−PEU interactions in order to comprehend their specific surface characteristics.

Introduction

Polyurethanes contain a repeating urethane linkage and have alternating hard (glassy or crystalline) and soft (elastomeric) segments. Typically, segmented polyurethanes exhibit a two-phase microstructure, which is promoted by the chemical incompatibility between the hard and soft segments. Factors affecting the degree of phase separation are hydrogen bonding, segment length, crystallinity, composition, and the mechanical and thermal history of the polyurethane.[1−3]

Wilkes and Yusek studied the bulk domain structure of polyurethanes and observed submicron-sized hard segment domains dispersed in a continuous rubbery soft segment matrix.[4] They proposed a model of hard segment rods packed in parallel and arranged in an orderly manner that they suggested might maximize hydrogen (H)-bonding.[4] H-bonding involves the N−H group in the urethane or urea as a proton donor and the carbonyl of the urethane or ether as the proton acceptor.[1] It has been shown that a urea carbonyl can H-bond to two N−H groups, which results in three-dimensional H-bonding that leads to unusually strong hard domain cohesion.[5,6]

Studies on the surface of poly(urethane urea) elastomers using infrared spectroscopy have shown that the N−H absorption peak was nearly completely H-bonded, which attests to the high degree of H-bonding within polyurethanes.[7] The nature and distribution of the H-bonded structure at polyurethane surfaces are believed to have a significant effect on protein adsorption and subsequent coagulation events in blood/material interfacing systems.[7] Consequently, many approaches have been studied in order to modify the surfaces and subsequently manipulate specific blood and cellular protein interactions with polymer surfaces. An example of a system of particular interest involves the interactions between enzymes and polyurethanes during degradation processes. Since most pitting and cracking associated with biodegradation occurs within the top 20 μm of the polyurethane surface,[8] surface modification is an ideal technique for improving the performance of polyurethanes in biomedical applications without affecting the bulk properties of the material.

Fluorinated polymers have attracted interest as a surface-modifying strategy because of their low surface energy, relative blood compatibility, lubricity, nonstick behavior, and thermal and oxidative stability.[9] The incorporation of fluorine in a phase-segregated polymer has been shown to result in the exposure of the fluorine group at the surface, which significantly increases the advancing water contact angle.[9−11] Fluorinated surface-modifying macromolecules (SMMs) were developed[12,13] and shown to reduce the hydrolytic degradation of base polyurethanes.[12] Despite the knowledge of their useful function, there has been very little information published which describes the specific interactions of the previously reported[12,13] fluorinated SMMs with their base polymer at the surface of the material. More specifically, there have been no studies to date that have probed the surface in order to determine the influence of these fluorinated SMMs on the microdomain surface structure of the native PEU. It is thought that the migration mechanism of polymeric additives such as the above fluorinated SMMs depends on the molecular weight of the molecule, the nature of the interactions between the base polymer and the additive, and the difference in chemical potential created at the interface between the polymer blend and the phase in contact with the polymer (i.e., air, water, blood, etc.).[14]

† Department of Chemical Engineering and Applied Chemistry.
‡ Institute of Biomaterials and Biomedical Engineering.
§ Department of Biomaterials, Faculty of Dentistry.
* To whom all correspondence should be addressed. Phone (416) 979-4903 ext 4341; Fax (416) 979-4760; e-mail paul.santerre@utoronto.ca.

10.1021/ma010283v CCC: $22.00
Published on Web 12/27/2001

Table 1. SMM Nomenclature

the first sequence of letters represents the oligomeric polyol used in the SMM	PTMO	poly(tetramethylene oxide) (M_w 1000 Da)
	PPO	poly(propylene oxide) (M_w 1000 Da)
the numeric sequence indicates the stoichiometric ratio of reactants in the SMM synthesis	322	3 diisocyanate 2 polyol 2 fluoro alcohol
	212	2 diisocyanate 1 polyol 2 fluoro alcohol
the final letter represents the type and fraction of fluoro alcohol used to end-cap the SMM prepolymer	L	low boiling fraction of B
	I	intermediate boiling fraction of B
Note: the mol wt of L < I ≅ F	F	intermediate boiling fraction of F
SMMs used in this study		PTMO-322I, PTMO-212I, PTMO-212F, PPO-212L

This study will attempt to obtain a broader understanding on the nature of fluorinated SMM structures at the surface of a base PEU. More specifically, the focus will be on investigating the influence of previously reported SMMs[12,13] and their blending on the nature of PEU phase structure as well as the effect of the SMMs on H-bonding interactions. This will be achieved by combining information from the following experimental methods: contact angle analysis, differential scanning calorimetry, atomic force microscopy, confocal microscopy, scanning electron microscopy, and attenuated total reflectance infrared spectroscopy.

Experimental Section

Synthesis of Base Poly(urethane urea). A base PEU was synthesized using 2,4-toluene diisocyanate (TDI, obtained from Aldrich Chemical Co., Inc., Milwaukee, WI), poly(tetramethylene oxide) (PTMO, M_w 1000 Da, obtained from DuPont Specialty Chemicals, Wilmington, DE), and ethylenediamine (ED, obtained from Aldrich) in a 2:1:1 stoichiometry. The details of the reaction procedure are described in previous work.[15]

Synthesis of Surface-Modifying Macromolecules. The SMMs were synthesized using 1,6-diisocyanatohexane (HDI, obtained from Aldrich, Milwaukee, MI), PTMO or poly(propylene oxide) (PPO, M_w 1000 Da, obtained from Aldrich, Milwaukee, MI), and two types of fluoro alcohols as end-capping agents. The two monofunctional fluoro alcohols were represented by the letters B and F (obtained from Van Waters & Rogers, Montreal, QB, Canada). B was an oligomeric chain made up of CF_2 units containing a terminal hydroxyl (average M_w 443 Da). F was a longer fluoro alcohol (average M_w 816 Da) that incorporated a poly(ethylene oxide) (PEO) spacer between the terminal hydroxyl and the CF_2 chain segment. Both fluoro alcohols were vacuum-distilled into low (L) and intermediate (I) distillation fractions. (The terminology refers to the relative temperature range from which they were collected.) The details of the fluoro alcohol preparation were described in other works.[16,17] In this study, the low and intermediate distillation fractions of B and the intermediate distillation fraction of F were used. The nomenclature for the four synthesized SMMs is given in Table 1.

The SMMs were synthesized using a two-step process, inducing a prepolymerization procedure followed by an end-capping reaction in a glovebox under dried nitrogen gas. The details of this synthesis have been reported in previous works.[12,13] The synthesis was carried out in *N*,*N*-dimethylacetamide (DMAc, Aldrich, Milwaukee, MI). The diisocyanate−polyol prepolymer was stirred for 3 h, and the temperature was maintained in the range 60−70 °C. The prepolymer was then cooled to 40 °C, and the fluoro alcohol was added dropwise to end-cap the prepolymer chains. 25 wt % excess fluoro alcohol was used in relation to the SMM stoichiometry. After stirring at room temperature overnight, the SMMs were precipitated into a 30 wt % solution of acetone in water to remove residual monomers. The oligomeric chains were then dried in a 60 °C oven under atmospheric pressure for 48 h and then at 7.5 mmHg for 24 h. Redissolving the material in DMAc, followed by filtering, precipitating, and redrying, further purified the SMMs. The SMMs were sealed in amber glass containers and stored in a desiccator at room temperature until required.

SMM Characterization. The polystyrene-equivalent molecular weight (M_w) of the PEU and the SMMs was determined by gel permeation chromatography (GPC). These methods have been previously reported in ref 15. The fluorine content of the SMMs was determined using standard elemental analysis techniques by Guelph Chemical Laboratories, Guelph, ON.

Differential Scanning Calorimetry. The thermal transitions of the individual polymers and the SMM−PEU blends were determined by differential scanning calorimetry (DSC). The SMMs were blended with the base PEU at a concentration of 4 wt %.[12] Films of the PEU base and the SMM−PEU blends were cast in Teflon molds from solutions of 5% w/v polymer in DMAc. The solvent was evaporated in an oven at 50 °C for 48 h, and the films were further dried in a vacuum oven for another 24 h at 7.5 mmHg. The films were approximately 0.3 mm thick. The 5−10 mg samples were cut from these films for DSC analysis. Because of their low molecular weights and poor handling properties, the pure SMMs could not be prepared by this method and were scanned in their uncast form.

DSC analysis was carried out at the Brockhouse Institute for Materials Research, McMaster University, Hamilton, ON, using a 2910 differential scanning calorimeter (TA Instruments, New Castle, DE). The polymer samples were cooled to −120 °C using liquid nitrogen. Data were collected at 20 °C/min from −120 to 220 °C for the base PEU and SMM−PEU blends and from −120 to 160 °C for the pure SMMs since thermogravimetric analysis of the SMMs indicated that the pure SMMs could start to degrade above 200 °C. Following the initial scan, the samples were immediately quenched from an amorphous state using dry ice and methanol and rescanned in accordance with methods reported by others.[18] The DSC profiles from the second scans are reported on in this study. Data analysis was performed using TA Instruments Thermal Analysis 2100 software.

Contact Angle Analysis. Contact angle analysis was carried out on films of the SMM−PEU blends in order to provide information on the relative hydrophobicity and the degree of modification achieved on the polymer surfaces. Unmodified PEU and SMM−PEU blend solutions were filtered using Teflon syringe filters and drop-cast on glass coverslips to form films that were approximately 0.15 mm thick. These films were dried in the same manner as the DSC films. Water was used as the probing liquid.

A standard goniometer apparatus was used to obtain the contact angles at the material−air interface (NRL contact angle goniometer, Ramé-Hart, Inc., Mountain Lakes, NJ). A bead of distilled, deionized water was introduced to the film surface with a microsyringe. The volume of this droplet was increased until the contact angle of the three-phase line remained visibly constant, indicating that the drop was large enough to overcome volume-dependent effects such as line tension.[19] The volume of a typical drop was approximately 20 μL. The contact angles on both sides of the drop were recorded as the advancing angle. The water was then slowly withdrawn from the droplet, until the contact angle again remained visibly constant. The contact angles on both sides of the droplet were recorded as the receding angles. This procedure was repeated

Table 2. SMM Characterization

SMM	M_w[a] (Da)	polydispersity	F content (%)
PTMO-322I	3.5×10^4	1.3	11.0
PTMO-212I	2.2×10^4	1.2	19.3
PTMO-212F	2.1×10^4	1.2	21.3
PPO-212L	1.9×10^4	1.2	18.0

[a] Polystyrene equivalent weight-average molecular weight.

for 10 water droplets. The statistical significance ($p < 0.05$) of the average contact angles was determined by analysis of variance (ANOVA).

Microscopy. Scanning electron microscopy (SEM) was performed to investigate the surface morphologies of the base PEU and the SMM−PEU blends. Films were cast and dried in the same manner as described above. The coated glass coverslips were mounted using double-sided adhesive tape and coated with platinum, which was deposited using an SC515 SEC coating unit (Polaron Equipment Ltd., England). The samples were imaged and photographed using a Hitachi S2500 scanning electron microscope (Hitachi Ltd., Mito City, Japan).

The polymer films were also analyzed using atomic force microscopy (AFM), which has been shown to provide topographical and phase information from a polymer surface.[20−22] TappingMode imaging (Digital Instruments, Santa Barbara, CA) was used to overcome problems associated with friction, adhesion, and electrostatic forces as well as avoid damaging the sample surface. This technique allowed for two- and three-dimensional topographic imaging of the PEU films, both base PEU and SMM−PEU blends. The polymer films were cast on circular glass coverslips (15 mm diameter) and dried as described above for the contact angle analysis. AFM was carried out at the Institute for Biomaterials and Biomedical Engineering, University of Toronto, Toronto, ON, using a Nanoscope Multimode IIIa microscope attached to a Nanoscope IIIa scanning probe microscopy controller (Digital Instruments, Santa Barbara, CA). Data analysis was carried out using specifically designed Digital Instruments software (version 4.23r2 Nanoscope software).

Confocal microscopy (CM) in reflectance mode was used to observe thin (1 μm) cross sections of the polymer films at the film surface and at material depths of 15 and 30 μm.[23] Films were cast on coverslips and dried as described above for contact angle studies. CM was carried out using an MRC-600 laser scanning microscope (Biorad Laboratories, CA) located at the Princess Margaret Hospital, Toronto, ON.

Attenuated Total Reflectance Infrared Spectroscopy. Attenuated total reflectance Fourier transform infrared spectroscopy (ATR-FTIR)[24] has previously been performed on PEUs[1] to investigate important surface properties relating to their infrared spectrum, including H-bonding characteristics and degradation.[5,25] The technique applied in this study assessed the nature of the chemical groups within the top 5 μm of the film surface using an IR beam with an incident angle of 45°. ATR-FTIR was performed on base PEU and the SMM−PEU blends at the Ontario Laser and Lightwave Research Centre, University of Toronto, Toronto, ON. Films were cast in Teflon molds and dried in the same manner as described above for DSC films. Strips of these films were cut and laid firmly in direct contact on the germanium crystal of the ATR mount for the FTIR spectroscope (Graseby Specac Ltd., Orpington, Kent, UK). The IR absorbance was measured from 700 to 4000 cm^{-1}. The scans were averaged to obtain a representative spectrogram for each sample. The curve deconvolution and analysis was carried out using Bomem Grams/386 software version 2.04 (Galactic Industrial Corp., Salem, NH).

Results

SMM Characterization. Table 2 shows the results of the elemental analysis and GPC for the pure SMMs. The M_w values for the SMMs ranged from 2.1×10^4 to 3.5×10^4 Da, and the polydispersities were between 1.2 and 1.3. These characteristics are consistent with previous syntheses for similar SMMs.[12] Because of differences in reaction stoichiometry, PTMO-322I had a higher soft segment content than the other SMMs. This resulted in a longer prepolymer chain length and accounts for the higher M_w of this SMM. All of the SMMs with 2:1:2 stoichiometries had similar M_w values ($\sim 2.0 \times 10^4$ Da) and fluorine contents ($\sim$20 wt %). PTMO-322I had a lower fluorine content (11 wt %) than the other SMMs as a result of having a longer prepolymer chain.

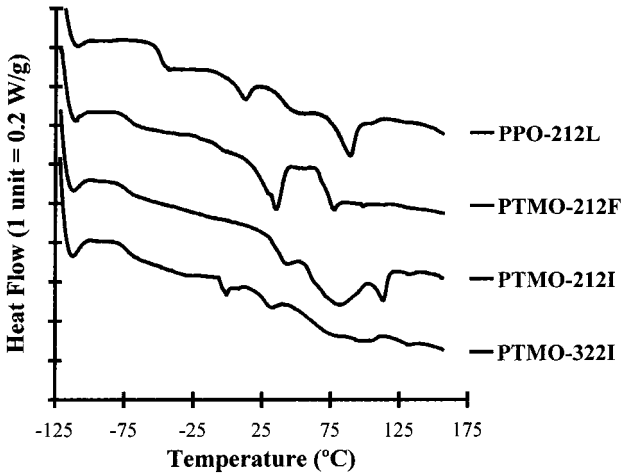

Figure 1. DSC thermograms of SMMs.

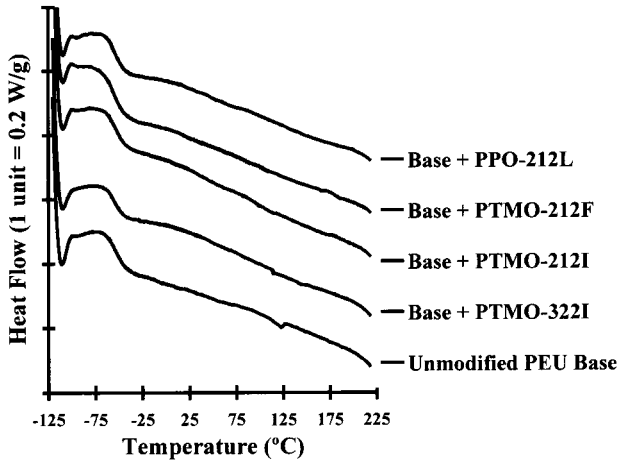

Figure 2. DSC thermograms of PEU base and SMM/PEU blends.

Figure 1 shows the DSC scans of the four SMMs. Glass transition temperatures (T_g) were observed for all of the SMMs. The PTMO-based SMMs exhibited this transition at approximately −74 °C, whereas the glass transition for PPO-212L was recorded at −49 °C. The widths of the glass transitions were all on the order of 10 °C. In addition to the T_g values, the SMMs with 2:1:2 stoichiometries showed prominent endotherms above the T_g's.

SMM−PEU Blend Characterization. The DSC analysis of the SMM−PEU blends is shown in Figure 2. The T_g of the base PEU (−55 °C) was not altered by the addition of any of the SMMs, which is consistent with the findings of other investigators using different base polymers.[12] The widths of these transitions were approximately 15 °C, and no SMM-related thermal transitions were observed in the blends.

Figure 3 shows the average advancing and receding contact angles of a water droplet on the surfaces of the

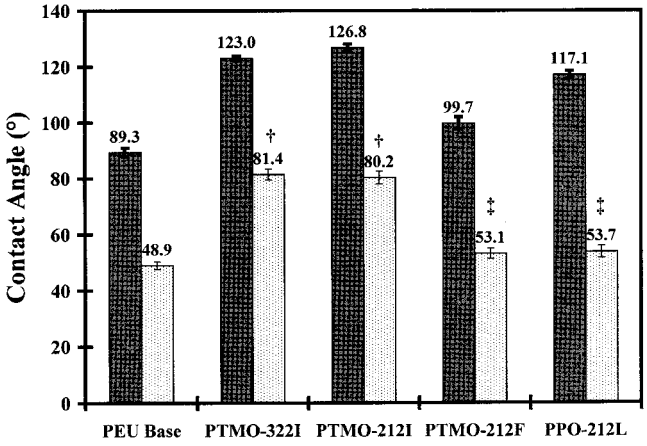

Figure 3. Contact angles of PEU base and SMM/PEU blends (error bars represent the standard deviation; † and ‡ symbols mark groups that are statistically similar for $p > 0.05$).

blend films. In all cases, the addition of the SMMs significantly increased both the advancing and receding contact angles over those of the base PEU. Statistical analysis also showed that both the advancing and receding contact angles of the PTMO-322I and PTMO-212I blends were significantly higher than those of PPO-212L, and all three of these blends showed higher advancing contact angles than the blend containing PTMO-212F. However, PTMO-212F and PPO-212L both exhibited statistically similar receding contact angles.

SMM−PEU Blend Microscopy. The SEM images of the surfaces are shown in Figure 4. At a magnification of 5K, minor surface features were apparent on some of these films. The PTMO-322I and PTMO-212F blends (Figure 4b,d) showed narrow ridges (long and narrow light shades) on the surface. The PPO-212L blend (Figure 4e) showed a dispersion of fine bumps (light shades), which was a unique observation among these films. The unmodified base PEU and the PTMO-212I blend (Figure 4a,c) were effectively featureless at this magnification. Despite these differences at the microscale, the surfaces were visually smooth.

Further analysis of the structure for the SMM−PEU blends was carried out using CM. These images are shown in Figure 5. The depth profiling capability of CM enabled imaging at 15 and 30 μm into the material as well as at the surface. The surface of the unmodified PEU (Figure 5a (i)) clearly shows different domains, shown as dark features (2−4 μm wide) amid a more dominant lighter phase. These dark domains are diminished in size but not in number at 15 μm beneath the surface, and at 30 μm into the material the sharp distinction between the phases has been lost. The PTMO-322I blend also shows isolated domains (dark regions) at the surface (Figure 5b (i)), but they are larger (3−7 μm wide) and their dispersion is less uniform than those in the base PEU. The lighter region is not as homogeneous as in the base PEU, suggesting some degree of domain mixing. The dark domains appear to be more diffuse at 15 μm beneath the surface, and by 30 μm into the material a finer, more regular pattern of light and dark domains is presented. The PTMO-212I blend has well-mixed phases at the surface (Figure 5c (i)), unlike either the base PEU or PTMO-322I blend. This pattern is consistent at both 15 and 30 μm into the material. The surface of the PTMO-212F blend (Figure 5d) is similar to that of the PTMO-212I blend, with the pattern reproduced at depths of 15 and 30 μm. The surface of the PPO-212L blend (Figure 5e) is also phase mixed, but the pattern is less regular than either the PTMO-212I or PTMO-212F blends. This blend shows increased phase blending through 15 and 30 μm into the material.

Figure 6 shows the three- and two-dimensional height images obtained by AFM. Cross-sectional height analysis (not shown) was performed using Digital Instruments software in order to determine the extent of height variation in each blend, the results of which are used to help contrast the differences between the blends. The unmodified PEU (Figure 6a) shows a relatively smooth surface with the exception of several broad, raised domains that are approximately 1 μm wide and 10 nm high. The blend with PTMO-322I (Figure 6b) shows significant height differences when compared to the unmodified PEU. There are gross topological features on the order of 3−7 μm in width (as viewed under lower magnification, not shown) that are raised approximately 500 nm. The height scans of the PTMO-212I blend (Figure 6c) show ridges that are about 1 μm wide and are elevated approximately 200 nm, whereas those of the PTMO-212F blend (Figure 6d) show many well-dispersed, small (300 nm wide, 10 nm high) features. There is also an underlying undulation to the surface with broad features having elevations of ~3 μm, which is particularly noticeable in the top left corner of the height images. The height images of the PPO-212L blend (Figure 6e) show elevations (2−3 μm wide, 10 nm high) that are similar in shape to those appearing in the unmodified PEU base. Apart from these broad features, the surface is relatively smooth.

SMM−PEU Blend Spectroscopy. Figure 7 shows the ATR-FTIR spectra of the carbonyl region for the unmodified PEU and the SMM−PEU blends. Several differences were noted in this region as well as in the amine region, which is shown in Figure 8. Peak assignment was carried out based on referenced peak assignments for polyurethanes,[5,25−30] and the actual peak analysis was determined by the deconvolution of the spectra as described in the experimental methods.

In the carbonyl region, the peak at 1731 cm^{-1} was attributed to nonbonded (or free) urethane groups and the 1711 cm^{-1} peak to H-bonded urethanes. The free urea peak appeared at 1692 cm^{-1}, and two peaks at 1660 and 1635 cm^{-1} were assigned to H-bonded ureas. These two bonded peaks result from the ability of the ureas to H-bond in different orientations. They have been defined as "short range" (1660 cm^{-1}) and "long range" or "three-dimensional" (1635 cm^{-1}) urea H-bonds.[5,31] On the basis of the data in Figure 7, it is apparent that the addition of SMMs has had an impact on the nature of H-bonding at the surface of the blends. Specifically, a noticeable increase in the free urea peak (1692 cm^{-1}, Figure 7) is seen for PPO-212L, PTMO-212F, and PTMO-212I blends. In addition, the size of the long-range H-bonded urea peak (1635 cm^{-1}, Figure 7) is reduced in the PTMO-212F and PTMO-212I blends relative to the short-range H-bonded urea peak. Notably, the addition of PTMO-322I to the PEU did not induce any obvious changes in the absorbance spectrum within the carbonyl region.

The amine groups appeared to be completely H-bonded, as no peaks are presented in the region attributed to free amines (around 3450 cm^{-1}, Figure 8).[5,32] This is consistent with previous studies on polyurethane elastomers[7] and is not altered by the presence of the

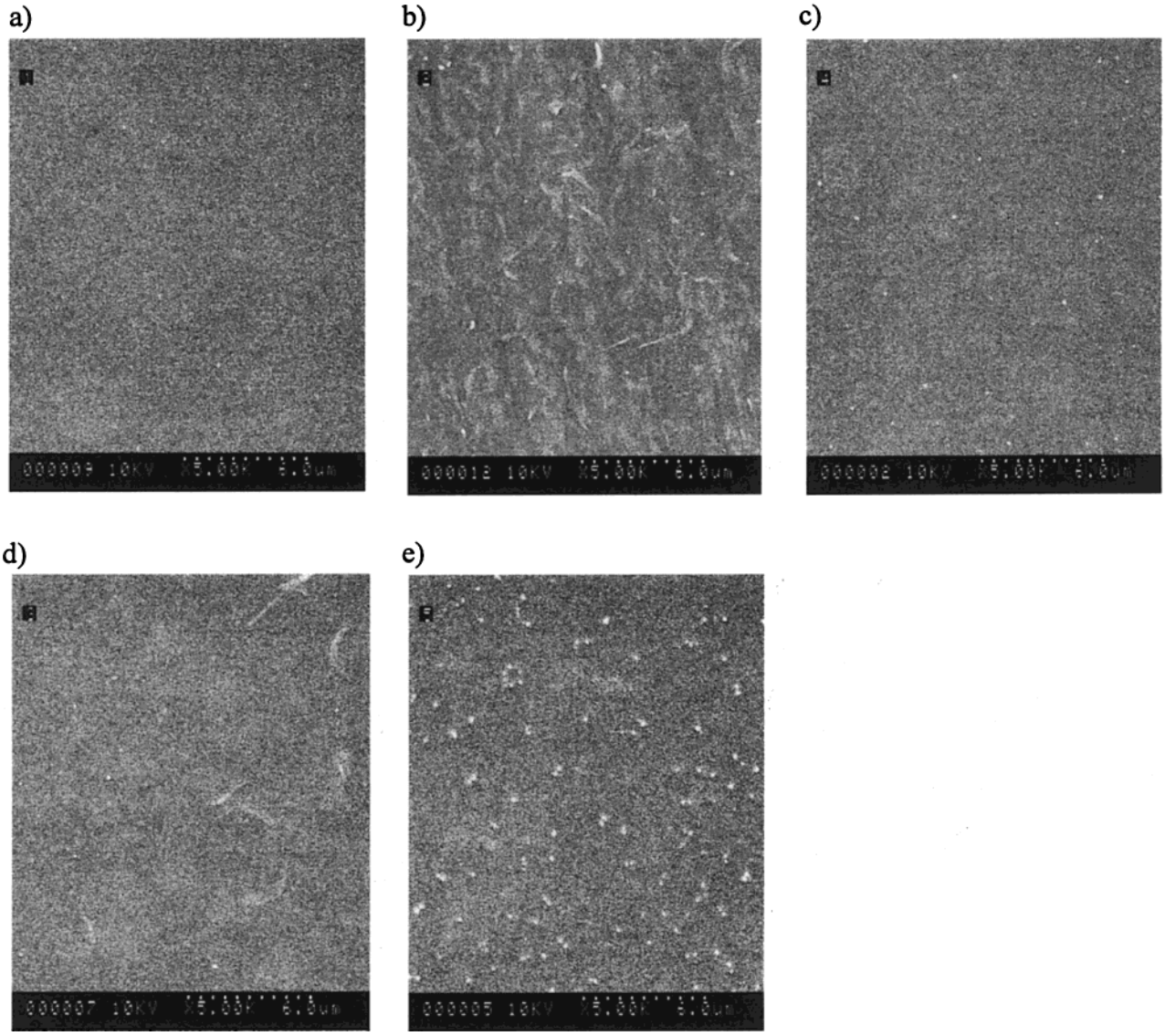

Figure 4. Scanning electron microscopy images of (a) unmodified PEU base and PEU base modified with (b) PTMO-322I, (c) PTMO-212I, (d) PTMO-212F, and (e) PPO-212L (image width = 17 μm).

SMMs. Spectroscopic wavenumbers have been attributed to specific types of amine H-bonding: the 3350 cm^{-1} area is representative of amine−carbonyl H-bonding, while H-bonding of ether oxygens with urethane or urea amines appears near 3320 and 3270 cm^{-1}, respectively.[29,30,32] As well as not inducing any changes in the spectrum for the carbonyl region (Figure 7), PTMO-322I did not noticeably affect H-bonding in the amine region (Figure 8). However, all of the 2:1:2 SMMs did augment the 3320 cm^{-1} (ether/urethane−amine bonding) and/or the 3350 cm^{-1} (carbonyl/amine bonding) peak area relative to that of 3270 cm^{-1} (ether/urea−amine).

Discussion

SMM Chemistry. The results indicate that substantial differences exist between the polymer blends in terms of their surface structure. The variations that were observed in the molecular weights, elemental compositions, and thermal transitions of the SMMs are attributable to differences in their chemistries. The variable that had the most pronounced affect on the molecular weight of the SMMs was the reaction stoichiometry, in that the 3:2:2 structure resulted in a higher polymer molecular weight oligomer. As anticipated, a higher molecular weight resulted in a lower fluorine content.

The T_g reflects the transition of the soft microphase from a glassy to rubbery state.[33] Taking into account the relatively low molecular weights of the fluorinated molecules, it would be anticipated that the SMMs would have T_g values relatively close to that of the oligomeric polyols. The PTMO-based SMMs showed T_g onsets at −78 °C, which correspond closely to the −79 °C T_g of pure PTMO.[17] However, while the T_g of PPO-212L appeared at −53 °C, the T_g of pure PPO is reported in the literature to be −70 °C.[34] This indicated that the PPO oligomer was more sensitive than the PTMO oligomer to the changes that resulted from the incorporation of the fluorine segments. The change could result from a weaker driving force toward separation of the different SMM segments (i.e., PPO and oligofluorocarbon) during polymer quenching.[18,35] The latter may be attributed to the shorter hydrophobic fluoro tail, which could be permitting easier mixing with the PPO segment, and/or steric hindrance by the methyl groups

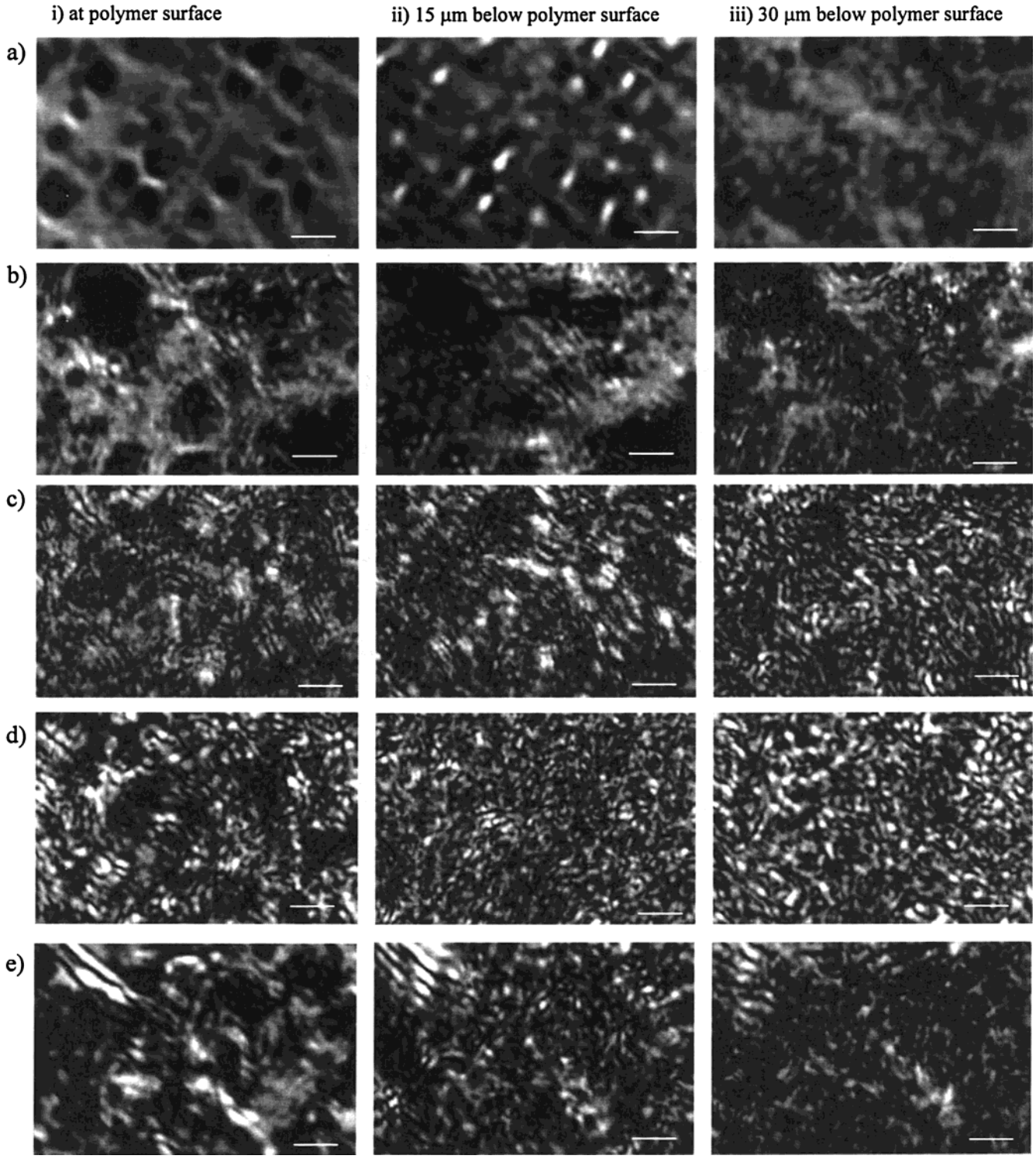

Figure 5. Confocal microscopy images of (a) unmodified PEU base and PEU base modified with (b) PTMO-322I, (c) PTMO-212I, (d) PTMO-212F, and (e) PPO-212L (white scale bar = 5 μm, image width = 38 μm).

of the polyol, which can inhibit packing and crystallization of the oligomeric diol chain segment.[36] In their studies of segmented polyurethanes, Chu and colleagues confirmed that phase separation was more complete in PTMO-based polyurethanes than in those with PPO−PEO soft segments.[37]

Additional thermal transitions were observed which were stronger for the SMMs synthesized with the 2:1:2 reaction stoichiometries than for PTMO-322I, suggesting the presence of more ordered structures in the former. Since previous studies have shown that the SMM concentration in the upper surface layer can be very high (in excess of 80 atomic % SMM),[12,13] the existence of ordered structures in these SMMs has some relative importance. If there are dense SMM phases within the upper surface layer of the blends, then some of the structures associated with the endotherms in Figure 1 may also be present at the surface of the blends.

The melting endotherms exhibited near 15 °C in PPO-212L and 40 °C in the PTMO-based SMMs reflect the melting temperatures of the respective polyols as indi-

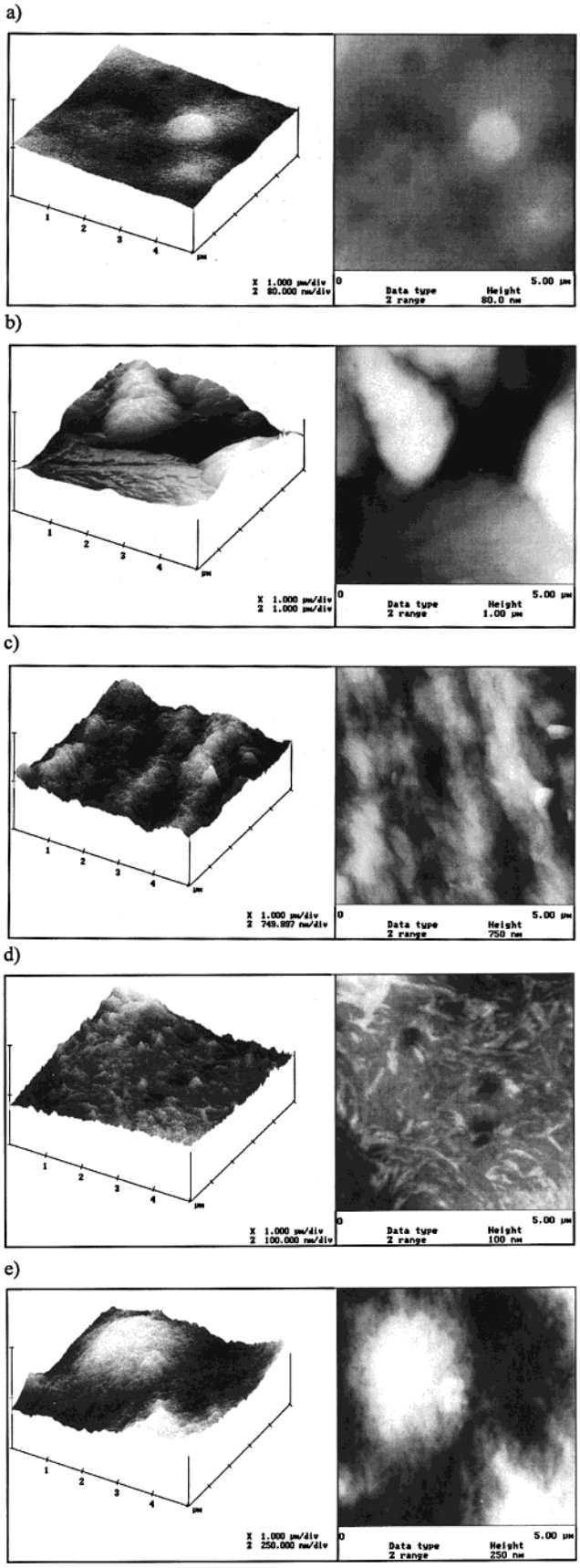

Figure 6. Atomic force microscopy images of (a) unmodified PEU base and PEU base modified with (b) PTMO-322I, (c) PTMO-212I, (d) PTMO-212F, and (e) PPO-212L (left = 3D height image, center = 2D height image; image width = 5 μm; lighter shading represents raised features).

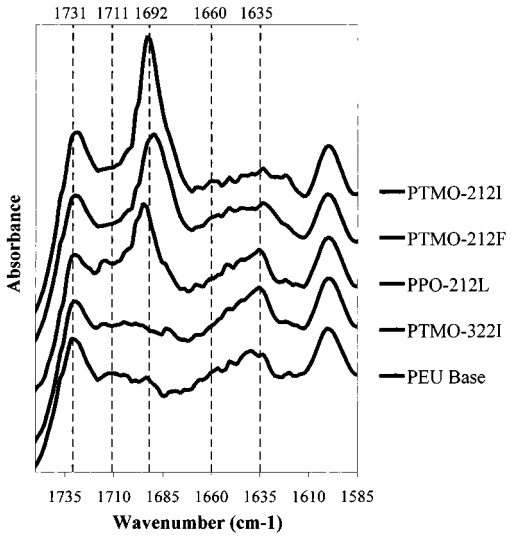

Figure 7. ATR-FTIR absorbance spectra for the carbonyl region of the unmodified PEU and the SMM/PEU blends.

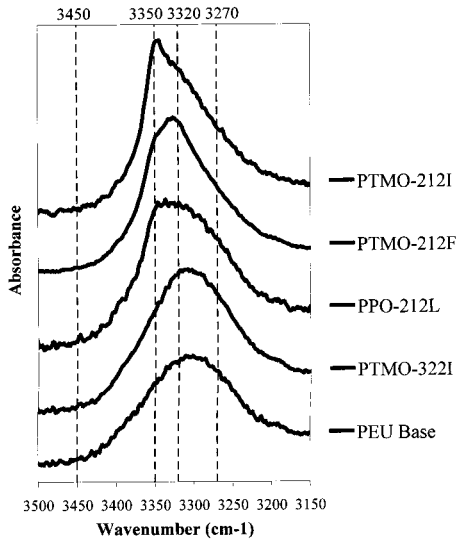

Figure 8. ATR-FTIR absorbance spectra for the amine region of the unmodified PEU and the SMM/PEU blends.

cated by manufacturer specifications. The polyol melting endotherm near 35 °C is particularly strong in PTMO-212F. The short PEO segments, which couple the HDI and fluoro tails in this SMM, are expected to enhance the chain flexibility, which in turn may facilitate the alignment of SMM chains. The end result of this process would be the formation of concentrated and ordered PTMO regions, thereby accounting for pronounced melting transition near 40 °C in this SMM. An endotherm also exists in PPO-212L (~90 °C) and PTMO-212I (~120 °C) that can be related to HDI melting as reported previously for polyurethanes.[38] It is also possible that the fluorine tails are contributing to the ordered structure, but there are no previous studies to support the association of transitions in this temperature range with oligomeric fluorocarbon segments. The higher melt temperature in PTMO-212I suggests that the ordering of HDI segments is greater in this SMM than in PPO-212L. This may result from the fact that the PTMO polyol in this SMM is more crystallizable than the PPO of PPO-212L, thus further excluding HDI segments from interactions with the PTMO segments. This analysis is in agreement with a more pure PTMO

phase observed by the T_g analysis. PTMO-212F does not exhibit a similar HDI melting endotherm as that observed for PTMO-212I and PPO-212L. This is believed to result from a perturbation of the structural ordering within the short HDI segments and is brought about by the flexible PEO chain that is immediately adjacent to the HDI segments.

PEU Bulk and Surface Modification by SMMs. Studies have shown that an increase in the phase mixing of poly(urethane urea) blends can be represented by an increase in the T_g of the soft segment.[35,39] In addition, the T_g width has been shown to reflect the phase heterogeneity.[40] Although only 4 wt % SMM was blended with the PEU, it has been shown in other work that the incorporation of a polyurethane into polystyrene at a 5 wt % loading was enough to induce a clear shift in the polystyrene T_g.[41] However, it should be noted that the latter example dealt with two materials having T_g values that were initially quite different from each other. In these blends, the incorporation of SMM into the PEU did not affect the onset temperature or width of the glass transitions, which indicated that SMM addition did not affect the bulk structure of the PEU to an extent detectable by DSC. Also, the presence of the SMMs did not induce any new thermal transitions to the bulk PEU, which is likely a reflection of the low SMM concentration.

Following the knowledge that the fluorinated SMM migrate and present themselves at the surface,[13,15] it is expected that fluorocarbon domains will exist at the polymer−air interface in order to minimize interfacial tensions.[11] The extent of this fluorine expression at the PEU surface is observed through contact angle analysis. In these polymer blend systems, the contact angle can be affected by the hydrophobicity of the area in contact with the three-phase line[42] as well as the reorientation of the surface due to water interactions with the more polar entity (i.e., urethane and urea linkages) of the material.[10,19] The advancing contact angle has been shown to be representative of the more hydrophobic domains of a surface, while the receding angle is affected predominantly by the hydrophilic domains.[42] Both the advancing and receding contact angles of PTMO-322I and PTMO-212I were significantly higher than those of the base PEU. This may be a reflection of the increased surface roughness of these two blends, as shown by AFM, which would hinder the movement of the three-phase line. The PTMO-212F and PPO-212L blends also have higher advancing and receding angles than the base PEU, but not as high as the other two SMM−PEU blends. In the case of PTMO-212F, surface reorientation would be expected to occur quickly if the hydrophilic PEO segments of the fluoro alcohol are free to orient themselves to the surface and interact with water. The rapid reorientation to a more hydrophilic surface would be expected to contribute to a lower receding contact angle when compared to the PTMO-322I and PTMO-212I blends. The lower advancing contact angle of the PPO-212L blend, as compared to that of the PTMO-212I blend, is suspected to be related to the good dispersion of small phase domains observed throughout the relatively smooth surface (Figures 4e, 5e, and 6e). The surface smoothness and finer phase heterogeneity would cause less hindrance to the advancing three-phase line, thereby lowering the measured contact angle relative to that of PTMO-322I and PTMO-212I. It should also be noted that other studies have shown that the presence of a shorter fluoro alcohol chain in the SMM has reduced both the advancing and receding contact angles of SMM/polyurethanes mixtures.[12]

Bonding Interactions at the SMM−PEU Blend Surfaces. The H-bonding interactions at the surfaces of the polymer films provide information that is suggestive of the manner by which surface modification was effected by the SMMs. The carbonyl and amine regions of the PEU spectrum provide a background against which the other blends can be compared. The presence of long-range (or three-dimensional) urea H-bonding at 1635 cm^{-1} in the base PEU spectrum (Figure 7) reflects an organized alignment of the chain-extended aromatic diisocyanate segments, which can be distinguished from urea−urethane carbonyl H-bonding at 1660 cm^{-1}. The broad peak in the amine region reflects the presence of all three types of H-bonding (described earlier) and supports the analysis of the carbonyl data.

The PTMO-322I blend does not show substantial differences from the base in either the carbonyl or amine regions. This indicates that there was likely very little disruption of the hard segment interactions in the base PEU. This was not unexpected, as the hard domains of the PEU and the ether regions of the SMM are relatively incompatible. Since the reaction stoichiometry of PTMO-322I yields a higher soft segment content and hence a higher ether content than the 2:1:2 SMMs, then it follows that mixing with the hard segment domains of the PEU will be more difficult. Given that the chemistries of the PEU base and this SMM are not substantially different from the perspective of the presence of carbonyl and amine groups, and since strong interactions between the two chemical groups were not observed within the SMM (as determined by thermal analysis, Figure 1), it is expected that there would not be considerable spectral differences between the blend and the base. The low level of SMM−PEU interactions and the lack of substantial PEU domain disruption suggests that poorly dispersed PTMO-322I-rich regions exist at the surface of the polymer blend. The relatively high level of heterogeneity would justify the higher contact angles observed for this blend (Figure 3).

The modification of the PEU with PTMO-212I led to large differences in the carbonyl and amine regions as compared to the base. The decrease in the long-range urea carbonyl H-bonding peak (1635 cm^{-1}) reflects a substantial disruption of the PEU hard segment domains within the surface layer studied. This explains the increase in the relative intensities of the short-range (1660 cm^{-1}) and free (1692 cm^{-1}) urea carbonyl peaks (Figure 7). The thermal analysis of this SMM indicated a high level of HDI ordering, implying that the urethane groups were able to undergo extensive interaction with themselves. Hence, it may be that the urethane groups of the SMMs were able to infiltrate the urethane and urea groups of the base and that these interactions are contributing to the changes in the urea peaks (Figure 7). The extent of PEU hard segment disruption indicated in the carbonyl region (i.e., 1692 cm^{-1}) suggested the presence of interactions between the HDI components of the SMM and the hard segment components of the PEU. This is also supported by the increased size of the amine−carbonyl peak at 3350 cm^{-1} in the amine region (Figure 8).

The changes in the carbonyl and amine H-bonding observed in the PTMO-212F blend were similar to those

discussed for the PTMO-212I blend. In the amine region (Figure 8), a shoulder is presented at the same wavenumber as the peak discussed for the PTMO-212I blend, which is believed to reflect interactions between SMMs as well as interactions between the HDI segment of the SMM with the hard segment of the base. However, PTMO-212F also exhibits a relatively larger peak near 3320 cm^{-1}. This peak has been attributed to interactions between urethane amines and ether oxygens, which suggests that interactions between the SMM and the polyol segments of the PEU are present as well as the aforementioned interactions. The confocal microscopy images for this blend (Figure 5d) showed a substantial change in domain dispersion which also supports the belief that there were significant SMM−PEU interactions.

The modification of the base PEU with PPO-212L led to very little disruption of the long-range urea carbonyl H-bonding relative to that of the pure base (Figure 7), but substantial changes in the free urea groups. This suggests that, unlike the other SMMs with 2:1:2 stoichiometries, PPO-212L does not infiltrate the PEU hard segments but instead interacts with the urea groups at the interface of domains. The relatively larger peaks near the amine region (3350 and 3320 cm^{-1}) reflect a reduction in the amount of urea/ether interactions associated with the native PEU material. The enhanced SMM−PEU interactions suggested by these observations are consistent with the high degree of domain blending presented by the confocal microscopy of this blend (Figure 5e). Therefore, PPO-212L shows unique H-bonding trends in that substantial interactions between the SMM and base PEU exist, unlike the PTMO-322I blend, but there is less disruption of the PEU hard segment in this blend as compared to the PTMO-212I and PTMO-212F blends.

Summary

The contact angle investigations and thermal analyses support the observation that the fluorinated SMMs of interest in this study migrate to the surface of the SMM−PEU blends, thereby lowering the surface energy with the surface expression of the fluoro tails without substantial changes to the bulk structure of the PEU. Although each of the SMM−PEU blends showed higher advancing contact angles, the increases observed for individual blends were not solely related to the masking of urethane groups with the hydrophobic fluorine tails but were also dependent on the microsurface roughness generated by the additive.

It was shown that, although each of the specific SMMs exhibited unique thermal transitions, the concentration of SMM added to the base PEU was not enough to induce new transitions in the bulk phase of the blends. However, the microscopy investigations clearly showed a wide range of phase blending at the surface of the various SMM−PEU systems. Furthermore, the phase blending patterns observed were found to reflect different types of H-bonding at the blend surfaces. Specifically, PTMO-322I did not interact substantially with the PEU and was also shown to exhibit poor blending with the native PEU domains. PTMO-212I and PTMO-212F established stronger interactions with the base, but the improved blending with the base was shown to result in PEU hard segment domain disruption. PPO-212L was unique in that it blended well with the PEU at the surface and formed interactions with the base but did not appear to interfere with H-bonding in the hard segment domains of the PEU surface. Previous studies by Santerre and Labow,[43] and more recently by Tang et al.,[44] have concluded that hard segment network stabilization reduces hydrolytic degradation. It is therefore hypothesized that the various interactions between the SMM and the PEU will influence the degree to which the SMM would be able to mask hydrolyzable groups in polyurethanes.

Finally, these investigations have shown that a wide variety of techniques including microscopy and ATR-FTIR spectroscopy are required to develop a thorough understanding of the nature of SMM presentation at a PEU surface.

Acknowledgment. The authors thank Robert Chernecky at the Faculty of Dentistry, University of Toronto, ON, for his SEM assistance. Financial support was provided by Materials and Manufacturing Ontario and the Ontario Ministry of Health.

References and Notes

(1) Lamba, N. M. K.; Woodhouse, K. A.; Cooper, S. L. *Polyurethanes in Biomedical Applications*; CRC Press LLC: New York, 1998.
(2) Sung, C. S. P.; Schneider, N. S. *J. Mater. Sci.* **1978**, *13*, 1689−1699.
(3) Gibson, P. E.; Vallance, M. A.; Cooper, S. L. In *Developments in Block Copolymers*; Goodman, I., Ed.; Elsevier Science: London, 1982; pp 217−259.
(4) Wilkes, C. E.; Yusek, C. S. *J. Macromol. Sci., Phys.* **1973**, *B7*, 157−175.
(5) Sung, C. S. P.; Smith, T. W. *Macromolecules* **1980**, *13*, 117−121.
(6) Wang, C. B.; Cooper, S. L. *Macromolecules* **1983**, *16*, 775−786.
(7) Grasel, T. G.; Cooper, S. L. *Biomaterials* **1986**, *7*, 315−328.
(8) McCarthy, S. J.; Meijs, G. F.; Mitchell, N.; Gunatillake, P. A.; Heath, G.; Brandwood, A.; Schindhelm, K. *Biomaterials* **1997**, *18*, 1387−1409.
(9) Chapman, T. M. *J. Polym. Sci., Part A: Polym. Chem.* **1989**, *27*, 1993−2005.
(10) Chapman, T. M.; Benrashid, R.; Marra, K. G.; Keener, J. P. *Macromolecules* **1995**, *28*, 331−335.
(11) Zhuang, H.; Marra, K. G.; Chapman, T. M.; Gardella, J. A., Jr. *Macromolecules* **1996**, *29*, 1660−1665.
(12) Tang, Y. W.; Santerre, J. P.; Labow, R. S.; Taylor, D. G. *J. Appl. Polym. Sci.* **1996**, *62*, 1133−1145.
(13) Pham, V. A.; Santerre, J. P.; Matsurra, T.; Narbaitz, R. *J. Appl. Polym. Sci.* **1999**, *73*, 1363−1378.
(14) Rosen, S. L. *Fundamental Principles of Polymeric Materials*, 2nd ed.; John Wiley & Sons: Chichester, 1993.
(15) Santerre, J. P.; Labow, R. S.; Duguay, D. G.; Erfle, D.; Adams, G. A. *J. Biomed. Mater. Res.* **1994**, *28*, 1187−1199.
(16) Ho, J.; Santerre, J. P.; Matsuura, T. *J. Biomater. Sci., Polym. Ed.* **2000**, *11*, 1085−1105.
(17) Tang, Y. W.; Santerre, J. P.; Labow, R. S.; Taylor, D. G. *J. Biomed. Mater. Res.* **1997**, *35*, 371−381.
(18) Hesketh, T. R.; van Bogart, J. W. C.; Cooper, S. L. *Polym. Eng. Sci.* **1980**, *20*, 190−197.
(19) Neumann, A. W.; Spelt, J. K. *Applied Surface Thermodynamics*; Marcel Dekker: New York, 1996.
(20) McGhie, A. J.; Tang, S. L.; Li, S. F. Y. *CHEMTECH* **1995**, *Aug*, 20−26.
(21) Reifer, D.; Windeit, R.; Kumpf, R. J.; Karbach, A.; Fuchs, H. In *Thin Solid Films*; Elsevier Science: Amsterdam, 1995; pp 148−152.
(22) Akhremitchev, B. B.; Mohney, B. K.; Marra, K. G.; Chapman, T. M.; Walker, G. C. *Langmuir* **1998**, *14*, 3976−3982.
(23) Herman, B.; Lemasters, J. J. *Optical Microscopy: Emerging Methods and Applications*; Academic Press: San Diego, 1993.
(24) Urban, M. W.; Craver, C. D. *Structure−Property Relations in Polymers, Spectroscopy and Performance;* Advances in Chemistry Series 236; American Chemical Society: Washington, DC, 1993.
(25) Marchant, R. E.; Zhao, Q.; Anderson, J. M.; Hiltner, A. *Polymer* **1987**, *28*, 2032−2039.

(26) Ning, L.; De-Ning, W.; Sheng-Kang, Y. *Polymer* **1996**, *37*, 3045−3047.
(27) Ning, L.; De-Ning, W.; Sheng-Kang, Y. *Polymer* **1996**, *37*, 3577−3583.
(28) Fare, S.; Petrini, P.; Motta, A.; Cigada, A.; Tanzi, M. C. *J. Biomed. Mater. Res.* **1999**, *36*, 62−74.
(29) Dillon, J. G. *Infrared Spectroscopic Atlas of Polyurethanes*; Technomic Publishing Company, Inc.: Lancaster, 1989.
(30) Teo, L.-S.; Chen, C.-Y.; Kuo, J.-F. *Macromolecules* **1997**, *30*, 1793−1799.
(31) Ning, L.; De-Ning, W.; Sheng-Kang, Y. *Macromolecules* **1997**, *30*, 4405−4409.
(32) Marand, E.; Hu, Q.; Gibson, H. W. *Macromolecules* **1996**, *29*, 2555−2562.
(33) Koberstein, J. T.; Galambos, A. F.; Leung, L. M. *Macromolecules* **1992**, *25*, 6195−6204.
(34) Santerre, J. P.; Brash, J. L. *J. Appl. Polym. Sci.* **1994**, *52*, 515−523.
(35) Takigawa, T.; Oodate, M.; Urayama, K.; Masuda, T. *J. Appl. Polym. Sci.* **1996**, *59*, 1563−1568.
(36) Wang, T. D.; Lyman, D. J. *J. Polym. Sci., Part A: Polym. Chem.* **1983**, *31*, 1983−1995.
(37) Chu, B.; Gao, T.; Li, Y.; Wang, J.; Despar, C. R.; Byrne, C. A. *Macromolecules* **1992**, *25*, 5724−5729.
(38) Tang, Y. W.; Santerre, J. P.; Labow, R. S. *J. Biomed. Mater. Res.* **2001**, *56*, 516−528.
(39) Grasel, T. G.; Homan, T. G.; Cooper, S. L. *Polym. Prepr.* **1987**, *28*, 40−41.
(40) Turi, E. A. *Thermal Characterization of Polymeric Materials*; Academic Press: San Diego, 1981.
(41) Theocaris, P. S.; Kefala, B. *J. Appl. Polym. Sci.* **1991**, *42*, 3059−3063.
(42) Dettre, R. H.; Johnson, R. E., Jr. *J. Phys. Chem.* **1965**, *69*, 1507−1515.
(43) Santerre, J. P.; Labow, R. S. *J. Biomat. Mater. Res.* **1997**, *28*, 1187−1199.
(44) Tang, Y. W.; Labow, R. S.; Santerre, J. P. *J. Biomed. Mater. Res.* **2001**, *57*, 597−611.

MA010283V